AIP Advances

An atomistic view on the Schottky barrier lowering applied to $SrTiO_3$/Pt contacts

Cite as: AIP Advances **9**, 045116 (2019); https://doi.org/10.1063/1.5082733
Submitted: 23 November 2018 . Accepted: 02 April 2019 . Published Online: 11 April 2019

C. Funck, and S. Menzel

View Online Export Citation CrossMark

ARTICLES YOU MAY BE INTERESTED IN

The physics and chemistry of the Schottky barrier height
Applied Physics Reviews **1**, 011304 (2014); https://doi.org/10.1063/1.4858400

Bulk electronic structure of $SrTiO_3$: Experiment and theory
Journal of Applied Physics **90**, 6156 (2001); https://doi.org/10.1063/1.1415766

Interplay between ferroelectric and resistive switching in doped crystalline HfO_2
Journal of Applied Physics **123**, 134102 (2018); https://doi.org/10.1063/1.5015985

AVS Quantum Science
Co-published with AIP Publishing
Coming Soon!

AIP Publishing

© 2019 Author(s).

An atomistic view on the Schottky barrier lowering applied to $SrTiO_3$/Pt contacts

Cite as: AIP Advances 9, 045116 (2019); doi: 10.1063/1.5082733
Submitted: 23 November 2018 • Accepted: 2 April 2019 •
Published Online: 11 April 2019

View Online Export Citation CrossMark

C. Funck[1] and S. Menzel[2,a)]

AFFILIATIONS

[1]Institute for Electronic Materials II & JARA-FIT, RWTH Aachen University, Sommerfeldstrasse 24, 52074 Aachen, Germany
[2]Peter Grünberg Institute 7 & JARA-FIT, Research center Jülich Wilhelm-Johnen-Strasse, 52425 Jülich, Germany

[a)]**Corresponding Author:** Stephan Menzel (st.menzel@fz-juelich.de)

ABSTRACT

The interface between a metal and a semiconductor is known as Schottky contact and a key factor in semiconductor technologies. Those interfaces normally build an energetic barrier, which is responsible for the exponential current voltage dependence. Analytical models often describe the right trend for the description of the Schottky barrier height, but fail to predict the barrier properties quantitatively correct. To overcome this problem atomistic and quantum mechanical approaches are required such as the here applied density functional theory combined with the non-equilibrium Greens function method. So far, these methods have rarely been applied to wide band gap metal oxides, which leads to a lack in the understanding of oxide electronics. The presented study deals with the image force induced Schottky barrier lowering of a $SrTiO_3$/Pt interface as a model system for wide band gap metal-oxide Schottky contacts. The Schottky barrier lowering is investigated for the case of different doping concentrations/positions and for different voltages. From a defect chemical point of view, oxygen vacancies act as donors in many metal oxides and dominate the electronic conduction in oxide electronics. Consequently, we investigated the Schottky barrier lowering induced by oxygen vacancies. The second doping mechanism is achieved in the sense of classical doping using Nb impurities, which form a conventional n-type donor. The atomistic simulation reveals the Schottky barrier lowering effect for both type of dopants. The results are compared to a standard analytical model regarding the Schottky barrier lowering.

© 2019 Author(s). All article content, except where otherwise noted, is licensed under a Creative Commons Attribution (CC BY) license (http://creativecommons.org/licenses/by/4.0/). https://doi.org/10.1063/1.5082733

I. INTRODUCTION

Metal semiconductor interfaces are crucial within many applications of electronic devices. Hence, the understanding of the physical and chemical phenomena at such interfaces is of great importance for the progress in semiconductor technologies. The class of wide band-gap metal oxides is of increasing interest in the new semiconductor application field of oxide electronics. The reason is the broad spectrum of promising properties and applications of metal oxides as gate dielectrics, capacitor based memories, resistive switching memories, ferroelectrics for catalytic applications.[1–21] Atomistic investigations regarding the quantum chemistry of the Schottky contact formation of these wide band-gap metal oxides compounds are still underrepresented and many questions remain open.[22–28] Experimentally, the current transport of these metal/oxide Schottky interfaces show an exponential voltage dependence. In the past, analytical expressions have been derived, which connects the current transport to fundamental material properties of the metal and the semiconductor. One example is the determination of the Schottky barrier height by the so called Schottky-Mott rule, which suggests that the Schottky barrier is the result of the difference between the work function in the metal and the electron affinity of the semiconductor. This theoretical rule describes correctly the trend of the Schottky barrier height for different metal/semiconductor systems. Besides the general trend that higher metal work functions lead to higher Schottky barriers, the rule cannot be confirmed quantitatively. Here, quantum chemical mechanism come into account as soon as a significant atomic orbital overlap arises at the Schottky interface, as it has been excellently reviewed by R. T. Tung.[29] Furthermore, the scaling of electronic devices reaches the nanometer scale and classical laws lose their validity. Therefore, atomistic methods are required such as density functional theory (DFT).[30,31] Today, the focus of existing DFT studies is mainly on covalent bonding semiconductors to investigate the quantum chemical processes of Schottky barrier

© Author(s) 2019

formation. Besides the formation of the Schottky barrier itself, there are also effects that lead to a lowering of the Schottky barrier, as the so-called image force induced Schottky barrier lowering. In this mechanism, an electron approaching the Schottky interface induces a screening mirror charge, which leads to attractive forces and a lowering of the Schottky barrier.[32] Similar to the Schottky-Mott rule, an analytical expression has been derived, to connect the Schottky barrier lowering with the material properties. The derivation of this analytical expression is based on classical electrostatics and connects the Schottky barrier reduction with the electric field. By using the maximum electric field it leads to the analytical equation

$$\Delta\phi(V,N) = e\left[\frac{e^3 N|(V_{\text{in}} - V)|}{8\pi^2\varepsilon_0^3\varepsilon_r^3}\right]^{1/4} \quad (1)$$

for the Schottky barrier lowering.[32] In equation (1), N is the doping concentration, V is the electrostatic potential $\varepsilon_0\varepsilon_r$ is the permittivity of the semiconductor, e is the elementary charge, V_{in} is the built-in potential defined by the difference of the bulk conduction band level and the Schottky barrier height.[32] Especially Schottky contacts based on a high work function material and a wide band gap intrinsically form a high built-in potential/high electric field. In the presence of such high fields, the electrostatic considerations leading to the Schottky barrier lowering according to equation (1) are not valid anymore. For instance, the high electric fields shift the position of the Schottky barrier less than 1 Å in front of the metal contact. This leads to a significant orbital overlap and quantum mechanical processes dominate the formation of the electronic structure. Thus, quantum mechanical methods are required. Details on this discussion are shown in the supplementary material. Unfortunately, the barrier lowering according to equation (1) is rarely investigated by means of quantum mechanical methods, which leads to the question whether equation (1) still gives meaningful results. So far, only a few studies exist that investigate directly or indirectly the modification of the barrier lowering due to a change in the doping or a change in the applied voltage. These studies are mostly related to silicon as well-known covalent bonding semiconductor.[33–36] This effect is experimentally analyzed in the work of Schafranek et al. using a $SrTiO_3$/Pt Schottky contacts with Nb-doping conditions and oxygen vacancy doping (reduced $SrTiO_3$) conditions.[37] They observe a significant change in the Schottky barrier for the case with and without oxygen vacancy doping from 0.5 eV to more than 1.2 eV. Jiao et al. showed that Schottky barrier lowering occurs in TiO_2 for different doping atom positions at zero bias.[36] A detailed study on the Schottky barrier lowering due to an external voltage stress is still lacking.

In this study, we investigate the Schottky barrier lowering of a $SrTiO_3$/Pt system with different types of dopants under an applied electric field using atomistic simulations based on DFT combined with the non-equilibriums Green's function (NEGF) formalism. We discuss whether equation (1) is a reasonable approximation for wide-band gap materials, whether it is still valid under non-dilute dopant concentrations and whether it is still valid for ultimately scaled devices. $SrTiO_3$ is an established wide band gap ionic semiconductor with many potential application fields and serves here as a model system for oxide electronics. In addition, we investigate whether Schottky barrier lowering occurs beyond the classical electrostatic limit.

In contrast to semiconductors, two types of donor-like dopants are important in oxide electronics. An intrinsically chemically doping based on oxygen vacancies and a conventional doping scenario by an impurity atom on a regular lattice site. The defect chemistry of oxygen vacancies shows that oxygen vacancies form shallow defect states close to the conduction band in $SrTiO_3$, and hence act like a donor.[38–42] In many other oxides, oxygen vacancies form shallow donor like defect states, too.[43] Such point defects are unavoidable due to the physical laws of the thermodynamics and therefore named intrinsic doping. As a result, this intrinsic doping is important for understanding the electrical properties in electronic oxides and it is responsible for different observed physical phenomena.[12,44–50] As an example for the conventional impurity doping, we substitute a Ti atom with a Nb atom. The Nb atom contains one additional valence electron compared to the Ti atom and thus acts as n-type donor in $SrTiO_3$.[51,52]

II. METHODS

To describe the Schottky barrier lowering under an external applied voltage on atomistic level, we performed DFT+NEGF simulations as implemented in the code ATK 2017.12 with semi-periodically electrode boundary conditions.[34,53,54] The investigated atomic configurations are shown in Figure 1a for the Nb doped system and for the intrinsic V_O doped system. The arrows indicate the positions of the two Nb atoms and the single oxygen vacancy in the central device region. The third arrow indicates the position of the Nb atom in the electrode. Comparing to the supercell

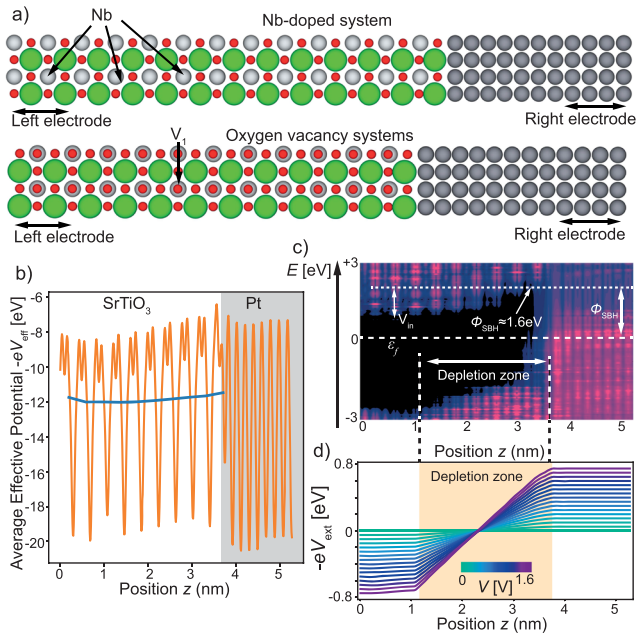

FIG. 1. In a) a sketch of the atomic structure is shown for the doping with one oxygen vacancy and the atomic structure for the case of Nb doped $SrTiO_3$. b) Shows the planar average effective potential (orange) and the macroscopic average potential (blue) for the case of zero bias and the atomic structure with V_O. c) Shows the LDOS of the configuration with V_O. d) Shows the internal voltage drop within the device for different external voltage bias.

© Author(s) 2019

volume of the central/device region this corresponds roughly to a doping concentration of $N \approx 9.3{\cdot}10^{20}$ cm^{-3} for both doping systems (one twofold ionizable oxygen vacancies and two single Nb impurity). The interface as shown in Figure 1a has been created with a Pt slab in [100] orientation and a $SrTiO_3$ slab with [100] orientation using the experimental lattice constant (a = 3.905 Å).[55] To match the small difference in the lattice constant, slight stress is put on the Pt slab.[56] The simulations are performed using a single zeta plus polarization local basis set including Troullier-Martins norm-conserving pseudopotentials as implemented in ATK.[57,58] The k-point sampling is adjusted to 5x5x100 (5x5x150) and the density mesh cutoff of 150 Ha for the oxygen vacancy (Nb-doped) systems. In advance to the non-zero bias simulations, all structures including the $SrTiO_3$/Pt interface have been relaxed below a force of 0.05 eV/Å using a 3x3x100 k-point sampling and a density mesh cutoff energy of 75 Ha with constrained electrodes. For the Nb-doped electrode system, the electrode slab itself contains one Nb impurity and has been relaxed below a force of 0.05 eV/Å prior to the relaxation of the complete structure. In all simulations, we used a Hubbard U of 6 eV on the Sr d-basis, the Ti-d basis, the O-p basis and the Nb-d basis in order to match the experimental band gap of 3.2 eV.[59] Due to the strong relation of the study to the resistive switching effect it is noted that for calculating the current voltage dependence not only the Schottky barrier lowering effect needs to be considered. Also electron-defect interactions are required, which maybe are not covered by DFT+NEGF.

III. RESULTS AND DISCUSSION

From the DFT+NEGF-calculations, it is possible to extract the three dimensional electrostatic effective potential. The planar average effective potential $\overline{\overline{V_{\mathrm{eff}}}}(z, V)$ is defined by the average over the xy-plane (perpendicular to the transport z-direction) for different externally applied voltages V. For the oxygen vacancy (V_O) doped system (see Fig. 1a), the planar average is shown as orange line in Figure 1b. From the planar average, the macroscopic average potential

$$V_{\mathrm{eff}} = \frac{1}{a_{\mathrm{STO}}} \int_{z-0.5a}^{z+0.5a} \overline{\overline{V_{\mathrm{eff}}}}(z)\,dz \tag{2}$$

in the $SrTiO_3$ layer is derived by averaging over one lattice constant. The macroscopic potential is plotted as blue line in Figure 1b. The macroscopic potential visualizes the band bending within the $SrTiO_3$.[34–36,60] Figure 1c shows the calculated local density of states (LDOS) for the V_O system.[34] In the bright purple region are many electron states and in the black region no states are present, i.e. the band gap. On the Pt side, many states are available at the Fermi-level confirming its metallic character. On the $SrTiO_3$ side, the black area confirms the semiconducting properties of $SrTiO_3$. The conduction/valence band of the $SrTiO_3$ can be defined by the colored states above/below the black band gap. By tracing the edge between the colored and the black region, the band bending can be roughly determined. It shows that a conduction band bending occurs from the $SrTiO_3$/Pt interface to the position of the oxygen vacancy, giving rise to the existence of a depletion zone, which is expected from classical semiconductor theory. Hence, the atomistic simulation results show the same properties as expected from classical semiconductor theory. We see this result as a validation for both, the established theory of Schottky contact formation and that our DFT simulation model is able to represent the electronic properties of the $SrTiO_3$/Pt contact. Next, we used DFT+NEGF to calculate the planar average potential at different voltages. This planar average effective potential allows to calculate the position dependent voltage drop $V_{\mathrm{ext}}(z, V)$ based on the externally applied voltage V by calculating the difference to the planar average potential at zero voltage $\overline{\overline{V_{\mathrm{eff}}}}(V = 0\mathrm{V})$ according to

$$V_{\mathrm{ext}}(z, V) = \overline{\overline{V_{\mathrm{eff}}}}(z, V) - \overline{\overline{V_{\mathrm{eff}}}}(z, V = 0). \tag{3}$$

A main requirement for the voltage induced Schottky barrier lowering is that the potential drop due to an external voltage occurs at the Schottky barrier, namely over the depletion zone. In Figure 1d, V_{ext} is plotted for different voltages V for the V_O system. The yellow background shows the depletion zone, which we extracted from the LDOS of Figure 1c. In contrast to the homogenously doped Schottky model with a voltage dependent depletion zone, the depletion zone obtained by DFT+NEGF is the distance between the dopant and the Schottky interface. The external voltage drop occurs uniformly within the Schottky depletion zone. In the simplified sense of an electronic equivalent circuit, this result suggests that the Schottky contact is the highest resistance in the system compared to the connecting electrodes (leads). The voltage drop for the other Nb-doped atomic configuration shows the same behavior (see supplementary material).

The Schottky barrier height is defined as the energetic distance between the (highest point in the) conduction band E_c and the position of the quasi Fermi-level in the metal electrode ε_f, leading to $\phi = E_c - \varepsilon_f$ (c.f. Fig. 1c). Both, conduction band and Fermi-level, change their energetic position under an external voltage V. Thus, the Schottky barrier lowering is based on a modification of the energetic distance between ε_f and the highest point of the conduction band E_c. Hence, these two parameters need to be considered for the barrier lowering. The shift of E_c can be extracted from the macroscopic potential, which is shown for different applied voltages in Figure 2a and b for the V_O and the Nb-doped system, respectively. The curve progression can be interpreted as the band bending at the Schottky contact. Both systems show exactly the same trends. The bands bend upwards towards the Schottky interface as it is expected from classical theory. Consistent with the classical theory, the bands in the doped $SrTiO_3$ region are forced downwards and the band bending increases with increasing reverse bias. As mentioned by Stradi et al, it is possible to locate the highest conduction band position simply by the highest value of the macroscopic potential named $E_h(V)$.[34] In Figure 2a and b, $E_h(V)$ is located close to the Pt electrode. Thus, it is approximated that the change of the highest point in the conduction band is equal to the change of the highest point in the macroscopic potential $\Delta E_h = E_h(V) - E_h(V = 0\ \mathrm{V})$, which can be extracted from the values in Fig. 2a/b. Second, the change of the Fermi-level position in the metal electrode is considered. In our simulations, the applied voltage is split equally by $\pm\ V/2$ to both electrodes (c.f. Fig 1d) and therefore the Fermi-level in the metal electrode shifts energetically upwards by $eV/2$. Taking together the change in the highest conduction band level (ΔE_h) and the upwards shift of the Fermi-level ($eV/2$), the change in the barrier lowering is obtained by the addition of both effects, i.e.

© Author(s) 2019

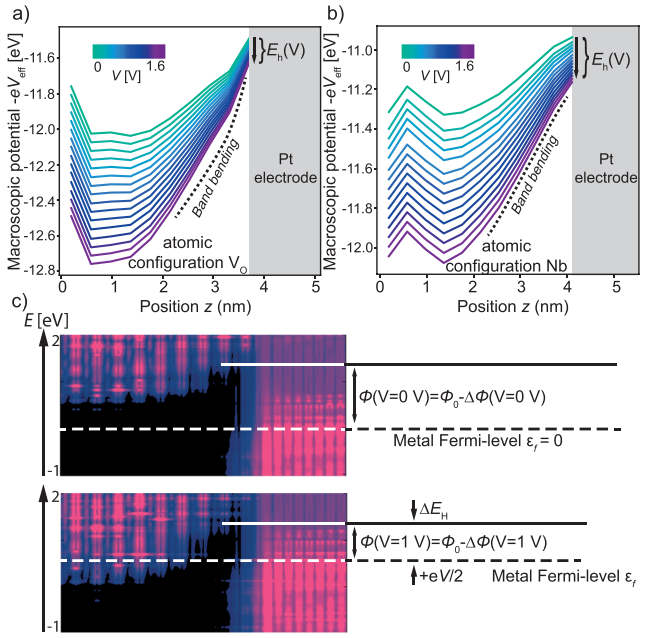

FIG. 2. a) The macroscopic potential of the vacancy configuration bias in the $SrTiO_3$ slab for different external voltages in reversed Schottky direction. b) The macroscopic potential of the Nb-doped configuration bias in the SrTiO3 slab for different external voltages in reversed Schottky direction. c) The local density of states for two different voltages indicating the change of the Schottky barrier lowering.

$\Delta\phi(V \neq 0) - \Delta\phi(V = 0) = \Delta E_h + eV/2$. This effect must also be visible in the LDOS. Therefore, we plotted the LDOS of the V_O system under two different voltages in Figure 2c and marked the important energy shifts. It shows how the Fermi-level shifts upwards due to the applied voltage by $eV/2$. The conduction band lowering by ΔE_h is only roughly visible, because it is difficult to define the highest point of the conduction band using this method. Nevertheless, the analysis of Figure 2a/b shows that quantum mechanical simulations predict a Schottky barrier lowering effect on the atomic scale. The barrier lowering determined by analyzing the LDOS at different voltage is consistent with the lowering calculated by the effective potential method (see supplementary material). In Fig. 3, we plotted the change in the Schottky barrier lowering $\Delta\phi(V) - \Delta\phi(V = 0\ V)$ for the V_O-doped system and the Nb-doped system. Both show the same trend in their curve progression, but a higher lowering is observed in the Nb-doped system, which may result from the higher built-in potential. Finally, we want to test whether the analytical equation (1) and the DFT+NEGF simulations lead to the same trend. It shows that the barrier lowering increases monotonously by increasing the external voltage. To calculate the barrier lowering according to equation (1), the built-in potential V_{in}, the permittivity and the dopant concentration are required. For the V_O doped system, the built-in potential V_{in} is extracted from the LDOS in Figure 1d as 1.1 V. The high frequency optical dielectric constant of $SrTiO_3$ is set to 5 in accordance with literature data.[61–63] The change of the barrier lowering $\Delta\phi(V) - \Delta\phi(V = 0\ V)$ according to equation (1) is plotted for the doping range N=10^{21}-10^{23} cm^{-3} in Fig. 3.

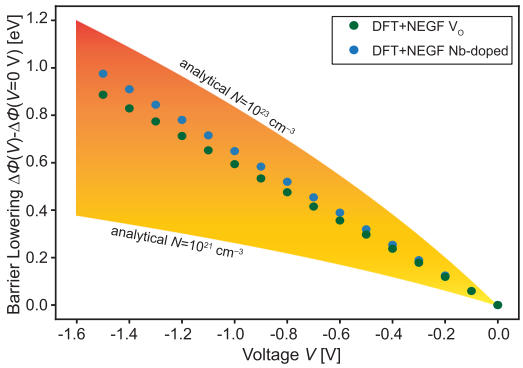

FIG. 3. Schottky barrier lowering due to the analytical equation 1 and according to the two different configurations.

As a direct conclusion, it can be seen that the analytical equation based on classical electrostatic suggests values in the same order of magnitude as the quantum mechanical approach. This is a remarkable result, considering that the classical electrostatic approach loses its physical validity to predict the Schottky barrier lowering under high electric fields (c.f. supplementary material). Hence, the analytical approach is able to give a meaningful estimation beyond its physical valid range. This bears the key massage that an assessment of the Schottky barrier lowering is still possible. Nevertheless, some differences appear in the results of the analytical and quantum mechanical approach. Hence, it is important to discuss several limits and shortcomings of both methods, which need to be considered when analyzing and interpreting the presented results. In the numerical description, we suggested that the DFT simulation has a doping concentration of $9.3{\cdot}10^{20}$ cm^{-3}. Comparing this value with the analytical description, it shows that the DFT concentration is too low. The most probable reason is that the DFT simulation represent a fixed atomic configuration, which cannot be simply transferred to a statistical concentration N. For instance, shifting the position of the oxygen vacancy leads to a change in the Schottky barrier lowering, but would not change the concentration N (c.f. supplementary material). Additionally, the curve progression of both methods differ, which may also stem from investigating a fixed atomic configuration. It could also stem from the approximation of the maximum electric field in the derivation of equation 1, which also induces a systematic error. In addition, assumptions in the DFT calculations may induce uncertainties in the obtained Schottky barrier lowering results: To overcome the bandgap problem of DFT a Hubbard U has been applied to fit the experimental band gap. Using the same U and numerical parameters in previous publications the electronic transport properties are predicted correctly.[56] Comparing the electronic dispersion (band structure) of Ref. 56 with hybrid potential simulations in Ref. 64 it could be seen that the Hubbard U does not influence the electronic dispersion. Nevertheless, a vague uncertainty due to the bandgap problem remains in the quantitative comparison. Another mismatch may arise by extracting the change in the conduction band using the macroscopic potential. This method may suffer from the computational limit of a few hundred atoms and may misjudge the position of the conduction band. Nevertheless, the analysis of the LDOS shows a similar conduction band lowering.

© Author(s) 2019

This limitation of a few hundred atoms also prevents to investigate the Schottky barrier lowering under a statistical interpretation. Having in mind the discussed problems, it can be concluded that Schottky barrier lowering occurs beyond the classical limit and can be roughly estimated using the analytical classical electrostatic approach.

IV. CONCLUSION

In this study, we investigated the Schottky barrier lowering effect of the electronic oxide model system $SrTiO_3$/Pt for two different doping systems: self-doping by oxygen vacancies and conventional doping. The barrier lowering as predicted by classical electrostatics can be observed using quantum mechanical methods for both doping mechanisms. The barrier lowering can be extracted using the macroscopic average potential or the local density of states for different voltages. A comparison between classical electrostatics and quantum mechanics reveals that the Schottky barrier lowering is estimated lower than the DFT results suggested. Besides the mismatches of the two methods, it is possible to find important conclusions. First, we could confirm by quantum mechanical methods that even under high electric fields/non-diluted conditions in wide band gap oxide materials Schottky barrier lowering could be observed on the atomic scale. Second, we showed that the analytical expression and the quantum mechanical methods give quantitatively comparable results. Therefore, it is still possible to estimate the Schottky barrier lowering using classical electrostatic methods under non-diluted conditions.

SUPPLEMENTARY MATERIAL

See supplementary material for additional information for the motivation of the classical limit of calculating the Schottky barrier lowering and further information regarding the voltage drop in the Nb:$SrTiO_3$ system.

ACKNOWLEDGMENTS

The authors gratefully acknowledge the computing time granted for the project no. cjpgi70 by the JARA-HPC Vergabegremium on the supercomputer JURECA at the Forschungszentrum Jülich. Compare to J. u. l. S. Centre, Journal of large-scale research facilities, 4 (2018). The work was supported by the SFB 917. The authors acknowledge M. Lezaic, F. Gunkel, P. C. Schmidt, M. Martin for the discussion.

REFERENCES

[1] C. Liu and T. Tseng, J. Eur. Ceram. Soc. **24**, 1449 (2004).
[2] M. A. Haque, A. D. Sheikh, X. Guan, and T. Wu, Adv. Energy Mater. **7**, 1602803-1 (2017).
[3] Y. Li, Y. Weng, X. Yin, X. Yu, S. R. S. Kumar, N. Wehbe, H. Wu, H. N. Alshareef, S. J. Pennycook, M. B. H. Breese, J. Chen, S. Dong, and T. Wu, Adv. Funct. Mater. **28**, 1705657-1 (2018).
[4] D. V. Christensen, Y. Frenkel, P. Schuetz, F. Trier, S. Wissberg, R. Claessen, B. Kalisky, A. Smith, Y. Chen, and N. Pryds, Phys. Rev. Appl. **9**, 054004 (2018).
[5] G. D. Wilk, R. M. Wallace, and J. M. Anthony, J. Appl. Phys. **89**, 5243 (2001).
[6] M. Houssa, M. Tuominen, M. Naili, V. Afanas'ev, A. Stesmans, S. Haukka, and M. M. Heyns, J. Appl. Phys. **87**, 8615 (2000).
[7] H. Kim, S. Campbell, and D. Gilmer, IEEE Electron Device Lett. **18**, 465 (1997).
[8] L. Zhang, A. Janotti, A. C. Meng, K. Tang, C. G. Van de Walle, and P. C. McIntyre, ACS Appl. Mater. Interfaces **10**, 5140 (2018).
[9] J. Robertson, Eur. Phys. J. Appl. Phys **28**, 265 (2004).
[10] J. Niinisto, K. Kukli, M. Heikkila, M. Ritala, and M. Leskela, Adv. Eng. Mater. **11**, 223 (2009).
[11] M. Gutowski, J. Jaffe, C. Liu, M. Stoker, R. Hegde, R. Rai, and P. Tobin, Appl. Phys. Lett. **80**, 1897 (2002).
[12] R. Waser, R. Dittmann, G. Staikov, and K. Szot, Adv. Mater. **21**, 2632 (2009).
[13] A. Sawa, Mater. Today **11**, 28 (2008).
[14] J. J. Yang, M. D. Pickett, X. Li, D. A. A. Ohlberg, D. R. Stewart, and R. S. Williams, Nat. Nanotechnol. **3**, 429 (2008).
[15] I. H. Inoue, S. Yasuda, H. Akinaga, and H. Takagi, Phys. Rev. **77**, 035105 (2008).
[16] M. Lanza, Materials **7**, 2155 (2014).
[17] Ch. Walczyk, Ch. Wenger, R. Sohal, M. Lukosius, A. Fox, J. Dabrowski, D. Wolanski, B. Tillack, H.-J. Muessig, and T. Schroeder, J. Appl. Phys. **105**, 114103 (2009).
[18] R. Cohen, Nature **358**, 136 (1992).
[19] S. Starschich, S. Menzel, and U. Böttger, Appl. Phys. Lett. **108**, 032903-1 (2016).
[20] S. Starschich, D. Griesche, T. Schneller, R. Waser, and U. Boettger, Appl. Phys. Lett. **104**, 202903-1 (2014).
[21] T. S. Boescke, J. Mueller, D. Braeuhaus, U. Schroeder, and U. Boettger, Appl. Phys. Lett. **99**, 102903 (2011).
[22] Y. Dong, S. Wang, J. Chai, Y. Feng, and A. Huan, Appl. Phys. Lett. **86**, 132103-1 (2005).
[23] R. Arras, V. G. Ruiz, W. E. Pickett, and R. Pentcheva, Phys. Rev. B: Condens. Matter **85**, 5404 (2012).
[24] J. Goniakowski and C. Noguera, Interface Sci. **12**, 93 (2004).
[25] M. Mrovec, J. Albina, B. Meyer, and C. Elsaesser, Phys. Rev. B: Condens. Matter **79**, 245121-1 (2009).
[26] K. Cheng, N. Han, Y. Su, J. Zhang, and J. Zhao, Sci Rep **7**, 41771-1 (2017).
[27] X. Ma, X. Wu, Y. Wang, and Y. Dai, Phys. Chem. Chem. Phys. **19**, 18750 (2017).
[28] N. R. D'Amico, G. Cantele, C. A. Perroni, and D. Ninno, J. Phys. Condens. Mat. **27**, 15006-1 (2015).
[29] R. T. Tung, Appl. Phys. Rev. **1**, 011304-1 (2014).
[30] P. Hohenberg and W. Kohn, Phys. Rev. B: Condens. Matter **136**, B864 (1964).
[31] W. Kohn and L. J. Sham, Physical Review **140**, 1133 (1965).
[32] S. M. Sze and K. K. Ng, Wiley (2007).
[33] J. Kim, B. Lee, Y. Park, K. V. Murali, and F. Benistant, IEEE 226 (2015).
[34] D. Stradi, U. Martinez, A. Blom, M. Brandbyge, and K. Stokbro, Physical Review B **93**, 155302-1 (2016).
[35] H. Dixit, C. Niu, M. Raymond, V. Kamineni, R. K. Pandey, A. Konar, J. Fronheiser, A. V. Carr, P. Oldiges, P. Adusumilli, N. A. Lanzillo, X. Miao, B. Sahu, and F. Benistant, IEEE Trans. Electron Devices **64**, 3775 (2017).
[36] Y. Jiao, A. Hellman, Y. Fang, S. Gao, and M. Kall, Sci Rep **5**, 11374-1 (2015).
[37] R. Schafranek, S. Payan, M. Maglione, and A. Klein, Phys. Rev. B **77**, 195310 (2008).
[38] C. Mitra, C. Lin, J. Robertson, and A. A. Demkov, Phys. Rev. B: Condens. Matter **86**, 155105-1 (2012).
[39] C. Ohly, S. Hoffmann-Eifert, X. Guo, and R. Waser, J. Am. Ceram. Soc. **89**, 2845 (2006).
[40] Z. Hou and K. Terakura, J. Phys. Soc. Jpn. **79**, 114704-1 (2010).
[41] R. Moos, W. Menesklou, and K. H. Hardtl, Appl. Phys. A-Mater. Sci. Process. **61**, 389 (1995).
[42] R. Waser, J. Am. Ceram. Soc. **74**, 1934 (1991).
[43] C. Linderalv, A. Lindman, and P. Erhart, J. Phys. Chem. Lett. **9**, 222 (2018).
[44] F. Gunkel, S. Hoffmann-Eifert, R. A. Heinen, D. V. Christensen, Y. Z. Chen, N. Pryds, R. Waser, and R. Dittmann, ACS Appl. Mater. Interfaces **9**, 1086 (2017).
[45] A. F. Santander-Syro, O. Copie, T. Kondo, F. Fortuna, S. Pailhes, R. Weht, X. G. Qiu, F. Bertran, A. Nicolaou, A. Taleb-Ibrahimi, P. Le Fevre, G. Herranz, M. Bibes, N. Reyren, Y. Apertet, P. Lecoeur, A. Barthelemy, and M. J. Rozenberg, Nature **469**, 189 (2011).
[46] R. Meyer, A. F. Zurhelle, R. A. De Souza, R. Waser, and F. Gunkel, Phys. Rev. B **94**, 115408 (2016).

© Author(s) 2019

[47]C. Xu, H. Du, A. J. H. van der Torren, J. Aarts, C. Jia, and R. Dittmann, Sci. Rep. **6**, 38296 (2016).
[48]R. De Souza, F. Gunkel, S. Hoffmann-Eifert, and R. Dittmann, Physical Review B **89**, 241401 (2014).
[49]G. W. Dietz, W. Antpohler, M. Klee, and R. Waser, J. Appl. Phys. **78**, 6113 (1995).
[50]Y. Hikita, K. Nishio, L. C. Seitz, P. Chakthranont, T. Tachikawa, T. F. Jaramillo, and H. Y. Hwang, Advanced Energy Materials **6**, n/a (2016).
[51]E. Drozdz and A. Kolezynski, RSC Adv. **7**, 28898 (2017).
[52]X. Guo, X. Chen, Y. Sun, L. Sun, X. Zhou, and W. Lu, Phys. Lett. A **317**, 501 (2003).
[53]M. Brandbyge, J. Mozos, P. Ordejon, J. Taylor, and K. Stokbro, Phys. Rev. B **65**, 165401-1 (2002).
[54]J. Soler, E. Artacho, J. Gale, A. Garcia, J. Junquera, P. Ordejon, and D. Sanchez-Portal, J. Phys. Condens. Mat. **14**, 2745 (2002).
[55]V. S. Kumar and M. K. Niranjan, J. Appl. Phys. **115**, 173705-1 (2014).
[56]C. Funck, A. Marchewka, C. Baeumer, P. C. Schmidt, P. Mueller, R. Dittmann, M. Martin, R. Waser, and S. Menzel, Adv. Electron. Mater. **4**, 1800062 (2018).
[57]N. Troullier, J. Phys. Rev. B: Condens. Matter **43**, 1993 (1991).
[58]D. Hamann, Phys. Rev. B **40**, 2980 (1989).
[59]M. Capizzi and A. Frova, Phys. Rev. Lett. **25**, 1298 (1970).
[60]O. Sharia, K. Tse, J. Robertson, and A. A. Demkov, Phys. Rev. B **79** (2009).
[61]K. Kamaras, K. Barth, F. Keilmann, R. Henn, M. Reedyk, C. Thomsen, M. Cardona, J. Kircher, P. Richards, and J. Stehle, J. Appl. Phys. **78**, 1235 (1995).
[62]C. Koonce, M. Cohen, J. Schooley, W. Hosler, and E. Pfeiffer, Physical Review **163**, 380 (1967).
[63]Y. Du, M. Zhang, J. Wu, L. Kang, S. Yang, P. Wu, and Z. Yin, Appl. Phys. A Mater. Sci. Process. **76**, 1105 (2003).
[64]S. Piskunov, E. Heifets, R. I. Eglitis, and G. Borstel, Computational Materials Science **29**, 165 (2004).

© Author(s) 2019